AMERICAN SOCIETY FOR MICROBIOLOGY | Journal of Virology®

VACCINES AND ANTIVIRAL AGENTS

Impact of Type I Interferon on the Safety and Immunogenicity of an Experimental Live-Attenuated Herpes Simplex Virus 1 Vaccine in Mice

Derek J. Royer,[a] Meghan M. Carr,[a] Ana J. Chucair-Elliott,[a] William P. Halford,[b] Daniel J. J. Carr[a,c]

Department of Ophthalmology[a] and Department of Microbiology and Immunology,[c] University of Oklahoma Health Sciences Center, Oklahoma City, Oklahoma, USA; Department of Medical Microbiology, Immunology, and Cell Biology, Southern Illinois University School of Medicine, Springfield, Illinois, USA[b]

ABSTRACT Viral fitness dictates virulence and capacity to evade host immune defenses. Understanding the biological underpinnings of such features is essential for rational vaccine development. We have previously shown that the live-attenuated herpes simplex virus 1 (HSV-1) mutant lacking the nuclear localization signal (NLS) on the ICP0 gene (0ΔNLS) is sensitive to inhibition by interferon beta (IFN-β) *in vitro* and functions as a highly efficacious experimental vaccine. Here, we characterize the host immune response and *in vivo* pathogenesis of HSV-1 0ΔNLS relative to its fully virulent parental strain in C57BL/6 mice. Additionally, we explore the role of type 1 interferon (IFN-α/β) signaling on virulence and immunogenicity of HSV-1 0ΔNLS and uncover a probable sex bias in the induction of IFN-α/β in the cornea during HSV-1 infection. Our data show that HSV-1 0ΔNLS lacks neurovirulence even in highly immunocompromised mice lacking the IFN-α/β receptor. These studies support the translational viability of the HSV-1 0ΔNLS vaccine strain by demonstrating that, while it is comparable to a virulent parental strain in terms of immunogenicity, HSV-1 0ΔNLS does not induce significant tissue pathology.

IMPORTANCE HSV-1 is a common human pathogen associated with a variety of clinical presentations ranging in severity from periodic "cold sores" to lethal encephalitis. Despite the consistent failures of HSV subunit vaccines in clinical trials spanning the past 28 years, opposition to live-attenuated HSV vaccines predicated on unfounded safety concerns currently limits their widespread acceptance. Here, we demonstrate that a live-attenuated HSV-1 vaccine has great translational potential.

KEYWORDS HSV-1, T cells, antibody, cornea, mouse, neovascularization

Received 2 December 2016 **Accepted** 17 January 2017

Accepted manuscript posted online 25 January 2017

Citation Royer DJ, Carr MM, Chucair-Elliott AJ, Halford WP, Carr DJJ. 2017. Impact of type I interferon on the safety and immunogenicity of an experimental live-attenuated herpes simplex virus 1 vaccine in mice. J Virol 91:e02342-16. https://doi.org/10.1128/JVI.02342-16.

Editor Richard M. Longnecker, Northwestern University

Address correspondence to Daniel J. J. Carr, Carr@ouhsc.edu.

Strategies for vaccine development have transitioned largely from empirical to so-called "next-generation" or rational approaches during the past 2 decades, a shift largely driven by technological advances and a better understanding of how innate immunity influences the generation of adaptive protection (1, 2). Despite these breakthroughs, the average person still acquires multiple herpesvirus infections during childhood (3). A licensed vaccine, however, exists only for varicella-zoster virus (VZV) (4). The live-attenuated Oka vaccine for VZV is generally well tolerated and has significantly reduced the incidence of VZV infection, morbidity, and mortality in the United States (5, 6). Furthermore, epidemiologic studies indicate that acquisition of herpes simplex virus 1 (HSV-1) has shifted toward early to late adolescence in recent decades within the United States, potentially creating an opportunity to introduce an effective prophylactic HSV-1 vaccine into the childhood vaccine regimen (7). HSV vaccines have been tested in multiple clinical trials, but these studies have focused on protein subunit vaccines

and have been largely unsuccessful to date (7). Established studies show that inactivated HSV alone does not elicit sustained protective immunity in mice or humans (8–10).

Herpesviruses are often considered to be exclusively pathogenic due to their unmistakable negative impact on health. Complications arising from HSV-1 infection are indeed common. Though generally recognized to be the causative agent of "cold sores," HSV-1 is also associated with significant visual morbidity, is a common cause of viral encephalitis, and is now a leading cause of primary genital herpes among women of child-bearing age in the United States (7, 11–13). Such problems rightfully beg the question of whether a live-attenuated vaccine for HSV-1 is safe. However, experimental evidence suggests that some elements of our acquired virome—and herpesviruses specifically—exert an important, yet largely underappreciated, symbiotic impact on the immune system by bolstering protection against heterologous pathogens (14–17).

Many live-attenuated vaccines also confer beneficial heterologous effects associated with protection against divergent pathogens (18, 19). Live-attenuated vaccines activate the same innate pathways triggered during natural infection. This activation step results in the production of specific cytokines that regulate the generation and quality of ensuing adaptive immune responses (20). Type I interferon (IFN-α/β) is a potent cytokine elicited by viral infection that promotes an antiviral state and exerts an immunomodulatory potential to regulate antiviral T helper type-1 (Th1) adaptive immune responses (21, 22). Traditional adjuvants in licensed subunit vaccines do not efficiently induce IFN-α/β or consistently stimulate strong Th1 responses although recent developments in adjuvant discovery are promising (23, 24). Collectively, this evidence implies that there may be an immunologic compromise involved in favoring theoretically safer adjuvanted protein subunit vaccines over historically proven live-attenuated vaccines. Moreover, the premise of eliminating common viral infections with subunit vaccines may also have unexplored consequences impacting the developing immune system's response to subsequent encounters with pathogens.

Demand for insights into the protective immunologic mechanisms elicited by novel vaccines is at an all-time high. We have recently shown that an experimental prophylactic live-attenuated HSV-1 vaccine generates a highly efficacious humoral immune response that protects animals against a lethal challenge when it is administered systemically (25). This vaccine, termed HSV-1 0ΔNLS, lacks the nuclear localization signal (NLS) on the infected cell protein 0 (ICP0) gene. The ICP0 protein has been characterized as an efficiency regulator governing viral transactivation and evasion of intrinsic host antiviral defenses (26). Clinical concerns that currently limit implementation of attenuated replication-competent viral vaccines primarily include the unknown risks of vaccine-mediated disease and latent persistence. Here, we (i) characterize the immune response elicited by the attenuated HSV-1 0ΔNLS vaccine, (ii) explore implications for vaccine-mediated disease and latency, and (iii) investigate how loss of IFN-α/β signaling impacts the virulence of HSV-1 0ΔNLS. While ocular infection with the vaccine strain is utilized here to efficiently characterize immunogenicity and neurovirulence, ocular delivery of HSV-1 0ΔNLS as a mucosal vaccine is not being pursued in light of the success of systemic vaccination (25). Moreover, evidence from our lab shows that prophylactic systemic vaccination is more protective against ocular infection than direct ocular vaccination (unpublished observations). In this paper, we show that the experimental vaccine strain is highly attenuated *in vivo* yet induces an innate and adaptive immune response largely identical to that of infection with a fully virulent strain without producing clinical signs of disease.

RESULTS

HSV-1 0ΔNLS is hypersensitive to rapid IFN-α/β-mediated repression in the cornea. We have recently shown that the live-attenuated HSV-1 0ΔNLS strain is highly susceptible to IFN-β-mediated inhibition *in vitro* and functions as a highly efficacious prophylactic vaccine (25). Given the role of the ICP0 protein as a viral efficiency regulator and an antagonist of intrinsic host defenses in the nucleus during HSV-1

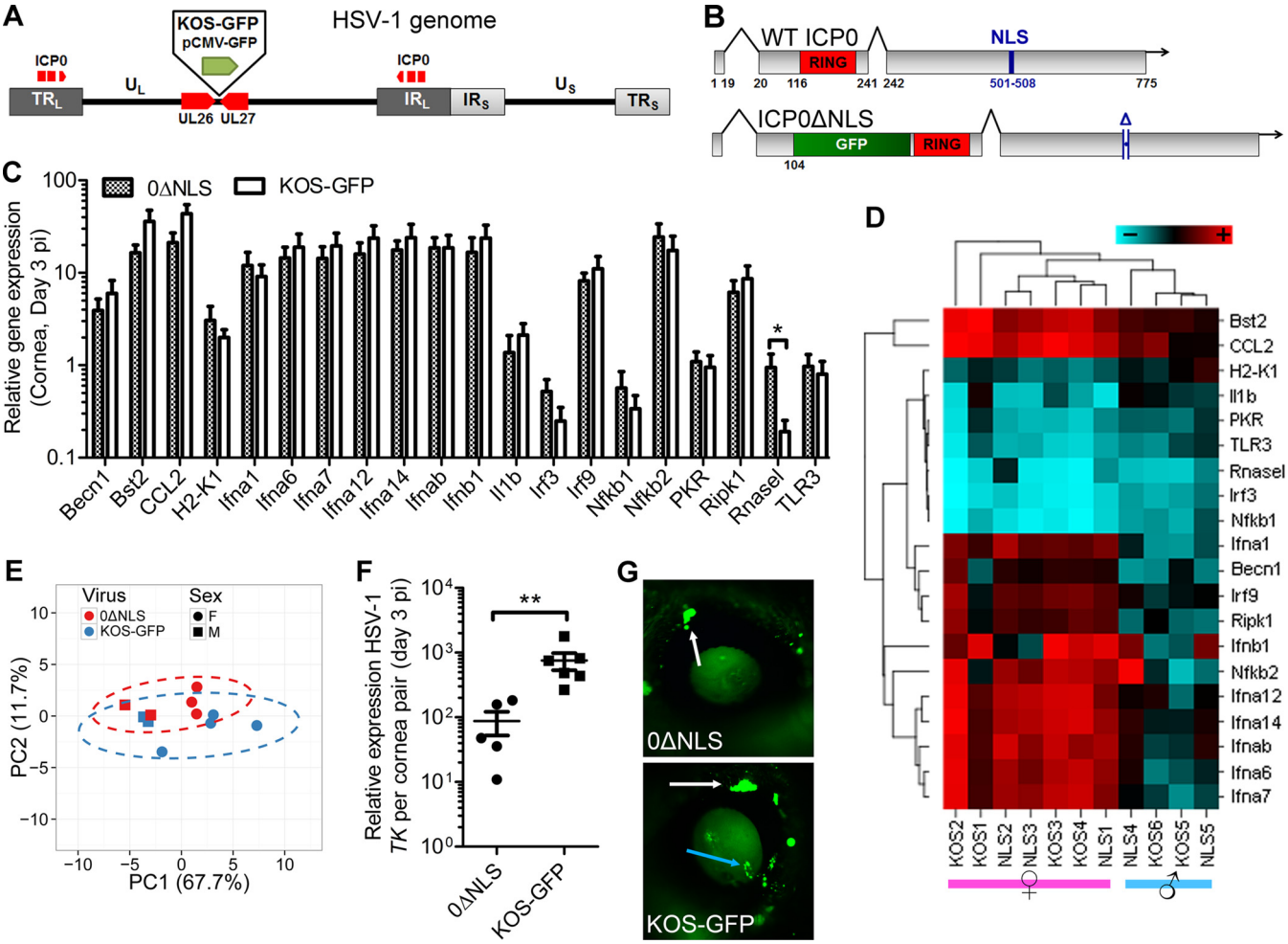

FIG 1 Cytosolic restriction of ICP0 and its impact on host antiviral responses. (A) Graphical representation of the linear HSV-1 genome. Landmark regions are denoted, including the terminal repeat (TR) and internal repeat (IR) sequences within the unique long (U_L) and short (U_S) genomic domains, as well as the gene coding regions for ICP0, UL26, and UL27. The pseudo-wild-type KOS-GFP virus contains an in-frame insertion of the green fluorescent protein coding sequence driven by a cytomegalovirus immediate early promoter (pCMV-GFP) between UL26 and UL27. (B) Graphical representation of the ICP0 coding sequences for the WT and 0ΔNLS strains. Landmark regions of the WT ICP0 coding sequence are denoted, including the RING finger E3 ubiquitin ligase structural domain on exon 2, and the nuclear localization signal (NLS) on exon 3. In the representation of the ICP0 coding sequence of the HSV-1 0ΔNLS strain, the canonical NLS signal peptide has been deleted, and a GFP coding sequence has been inserted in frame between codons 104 and 105 of the ICP0 gene. (C) Relative host antiviral gene expression in corneas of mice inoculated with 1×10^4 PFU of HSV-1 0ΔNLS or KOS-GFP at day 3 postinfection (p.i.) calculated by the $2^{-\Delta\Delta CT}$ method, with *GAPDH* (glyceraldehyde 3-phosphate dehydrogenase) and *TBP* (TATA box-binding protein) used as reference genes. Antiviral genes include beclin1 (*Becn1*), tetherin (*Bst2*), C-C motif chemokine ligand 2 (*Ccl2*), mouse major histocompatibility complex class II (MHC-II/H2-K1), IFN-α (*Ifn-α1,-α6, -α7, -α12, -α14*, and *-αB*), IFN-β (*Ifnb1*), interleukin-1β (*Il1b*), IFN regulatory factor 3/9 (*Irf3/9*), nuclear factor κB-1/2 (*Nfkb1/2*), protein kinase R (*Pkr*), receptor-interacting protein kinase (*Ripk*), RNase L (*Rnasel*), and Toll-like receptor 3 (*Tlr3*). (D) Heat map of the relative host gene expression levels organized by hierarchical clustering; extending dendrograms reflect similarities/relationships between variables. Animal sex is denoted below the graph. (E) Principal-component analysis of gene expression data with percentages of total variance indicated on the axes. (F) Relative expression of the early viral lytic gene thymidine kinase (TK) in the corneas of mice ocularly infected with 0ΔNLS or KOS-GFP at day 3 p.i., calculated as described above. (G) Representative images of infected corneas showing virus-encoded GFP fluorescence at a magnification of ×1.6 (*in vivo* imaging; the entire eye is shown for perspective). White arrows signify viral antigen in ocular discharge lining the lid margins. The blue arrow denotes viral lesions in the corneal epithelium observed in KOS-GFP-infected mice. Data reflect means ± SEM for 5 to 6 mice per group (3 independent experiments). *, $P < 0.05$; **, $P < 0.01$ (determined by Mann-Whitney *U* test).

infection (26), we hypothesized that the HSV-1 0ΔNLS virus would evoke a more potent antiviral gene signature *in vivo* than a pseudoparental strain (Fig. 1A, KOS-GFP) during acute infection due to the lack of the nuclear localization signal on ICP0 (Fig. 1B). Transcriptomic profiling of antiviral genes in the cornea following ocular infection with HSV-1 0ΔNLS or KOS-GFP (where GFP is green fluorescent protein) revealed little substantive difference in host gene signatures relative to those of the virus strain (Fig. 1C). Host genes surveyed included multiple type I IFN family members, innate signaling mediators, antiviral effectors, and autophagy-related transcripts. Genes were selected due to the well-established connections of their respective pathways to the host

defense against HSV-1 (27–29). The endoribonuclease RNase L was the only transcript noted to be differentially expressed in a comparison of the viral strains. Explicitly, RNase L expression was maintained during infection with HSV-1 0ΔNLS but was repressed in animals infected with HSV-1 KOS-GFP (Fig. 1C). The importance of the RNase L pathway in the host defense against HSV-1 via inhibition of protein synthesis and the ability of ICP0 to subvert its function are well established in certain cell types (27, 30–32).

Hierarchical clustering of the gene expression data revealed a discernible sex bias in the upregulation of IFN-α/β and autophagy-related transcripts, with expression levels higher in females (Fig. 1D). Principal-component analysis corroborated the lack of an outright difference in antiviral gene signatures among virus strains but supported the apparent sex bias as the male- and female-derived samples clustered separately along the primary principal component (Fig. 1E). Furthermore, the higher relative resistance of adult female mice to HSV-1 infection is noted in the literature (33–35) and is consistently supported in our empirical studies (unpublished observations). Our data provide compelling evidence that the sex bias in susceptibility could be mechanistically linked to a disparity in antiviral gene induction during acute infection. While the limited sample size admittedly restricts further inferences of sex bias in the host innate antiviral response to HSV-1, the impact on immunity of sex as a biological variable is a highly relevant topic (36).

Because no generalized differences in host antiviral gene signatures were observed corresponding to infection with HSV-1 0ΔNLS or KOS-GFP, we subsequently investigated viral fitness between the two strains *in vivo*. Levels of acute viral replication were initially compared by expression of the HSV-1 lytic thymidine kinase (TK) gene in paired corneas at day 3 postinfection (p.i.) (Fig. 1F). TK gene expression was approximately 10-fold lower in corneas infected with HSV-1 0ΔNLS than in those infected with KOS-GFP (Fig. 1F). This finding is consistent with our previous data showing that HSV-1 0ΔNLS is much more sensitive to IFN-β-mediated inhibition *in vitro* than the parental wild-type (WT) HSV-1 KOS strain (25). Furthermore, live-animal imaging showed viral antigen (i.e., virus-encoded GFP) in mucopurulent discharge surrounding the eyelid margins of both groups; however, viral lesions were evident only in the corneal epithelium of HSV-1 KOS-GFP-infected animals (Fig. 1G).

HSV-1 0ΔNLS lacks the neurovirulence of wild-type HSV-1. Viral neuroinvasion was assessed by plaque assay in the cornea-innervating trigeminal ganglia (TG) at day 3 p.i. In these experiments, infectious virus was detectable, albeit at low titers, in only 14% of TG specimens from HSV-1 0ΔNLS-infected C57BL/6 (WT) mice (Fig. 2A). The frequency of neuroinvasion increased to 80% at day 3 p.i. in WT mice infected with HSV-1 KOS-GFP (Fig. 2A). To complement this study and clarify the impact of IFN-α/β signaling on viral neuroinvasion, mice lacking the IFN-α/β receptor (CD118$^{-/-}$) were ocularly infected with HSV-1 0ΔNLS. In these experiments, virus was detected in ganglia from all CD118$^{-/-}$ mice by day 3 p.i. (Fig. 2A), thereby substantiating the extent to which HSV-1 0ΔNLS is repressed by IFN-α/β signaling *in vivo*.

We have previously shown that CD118$^{-/-}$ mice are highly susceptible to HSV-1 neuroinvasion and quickly succumb from encephalitis pursuant to ocular infection with HSV-1 McKrae (29, 37). However, HSV-1 McKrae exhibits greater neuroinvasiveness and pathogenicity than HSV-1 KOS *in vivo* (38–40). Nonetheless, all CD118$^{-/-}$ mice infected with HSV-1 KOS-GFP (1×10^5 PFU) by either the ocular or intranasal route expired by day 9 p.i. (Fig. 2B). Conversely, CD118$^{-/-}$ mice infected with HSV-1 0ΔNLS virus survived regardless of the inoculation route and exhibited no overt signs of neurological impairment (Fig. 2B). Lower ocular inocula of HSV-1 KOS-GFP in CD118$^{-/-}$ mice subtly delayed but did not reduce the frequency with which this infection produced a lethal outcome (Fig. 2C). Accordingly, the survival of the highly immunocompromised CD118$^{-/-}$ mice infected with HSV-1 0ΔNLS highlights the highly attenuated phenotype of this experimental vaccine strain.

The severity of neurovirulence associated with primary HSV-1 infection is dually dependent upon the proficiency of neuroinvasion from infected mucosal sites and the

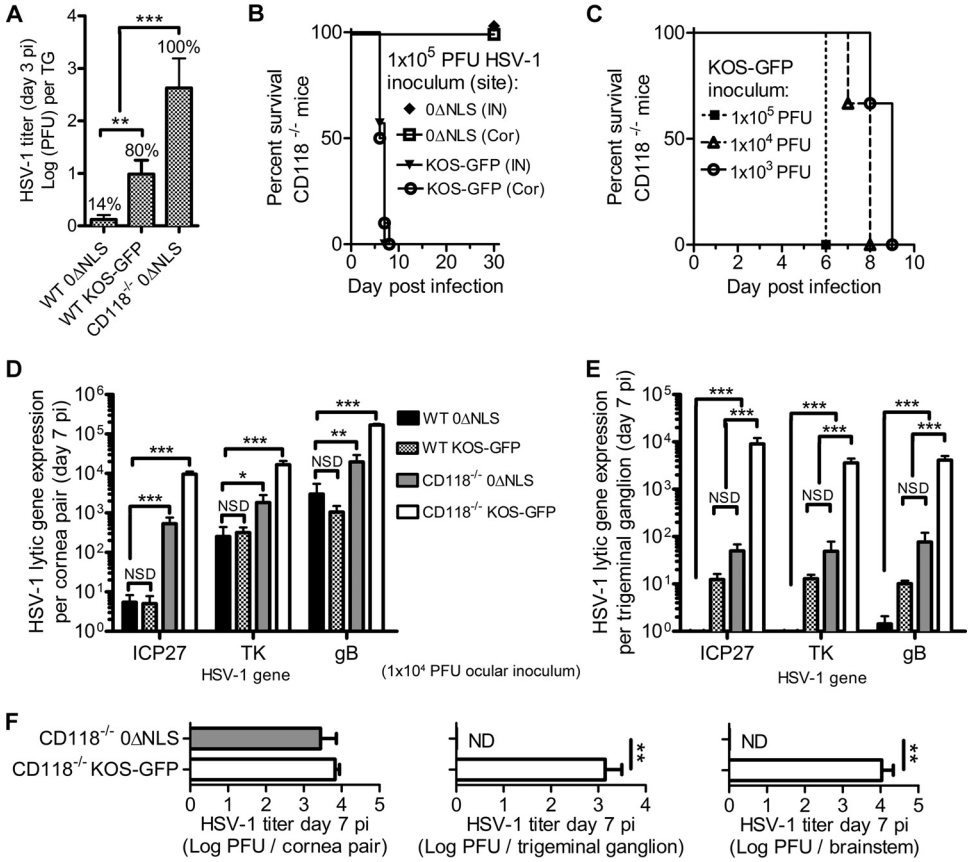

FIG 2 The 0ΔNLS mutation attenuates HSV-1 neurovirulence, even in the absence of IFN-α/β signaling. (A) Viral titers in the trigeminal ganglia (TG) of WT and CD118$^{-/-}$ mice ocularly infected with 1×10^5 PFU of HSV-1 0ΔNLS or KOS-GFP at day 3 p.i. Inset values indicate the percentages of samples with detectable virus ($n = 5$ to 14 samples per group, 3 to 4 independent experiments). (B) Survival of CD118$^{-/-}$ mice following ocular/corneal (Cor) or intranasal (IN) infection with 1×10^5 PFU of HSV-1 0ΔNLS or KOS-GFP ($n = 7$ mice/group, 2 independent experiments). (C) Survival of CD118$^{-/-}$ mice following ocular infection with various viral loads of HSV-1 KOS-GFP ($n = 3$ mice/group). (D and E) Expression of HSV-1 genes from each temporally regulated lytic gene class in the corneas and TG of WT and CD118$^{-/-}$ mice ocularly infected with 1×10^4 PFU of HSV-1 0ΔNLS or KOS-GFP ($n = 3$ to 5 mice per group, 2 independent experiments). (F) Viral titers in the corneas, TG, and brainstems of CD118$^{-/-}$ mice infected with 1×10^4 PFU of HSV-1 0ΔNLS or KOS-GFP at day 7 p.i. ($n = 3$ to 5 mice/group, 2 independent experiments). Note that titers of infectious virus were not detectable in WT mice at this time (data not shown). ND, not detected. Statistical differences were determined by one-way analysis of variance with Newman-Keuls multiple comparison tests. *, $P < 0.05$; **, $P < 0.01$, ***, $P < 0.001$; NSD not statistically different.

strain's subsequent replicative efficiency within the peripheral nervous system. While the HSV-1 KOS-GFP strain was substantially more neuroinvasive than HSV-1 0ΔNLS at early time points (Fig. 2A), viral titers were not detectable by plaque assay in the TG of WT mice infected with either HSV-1 0ΔNLS or KOS-GFP by day 7 p.i. (data not shown). This observation is consistent with previous reports using the HSV-1 RE strain, which exhibits virulence similar to that of the KOS strain in C57BL/6 mice (41, 42). On the basis of the above findings, the dynamics of virulence were investigated further in corneas and TG by profiling viral lytic gene expression at day 7 p.i. in WT and CD118$^{-/-}$ mice. At this time point, low-level to moderate viral replication was detected in the corneas of WT mice infected with HSV-1 KOS-GFP and 0ΔNLS (Fig. 2D). Viral replication persisted at similar levels in the TG of WT mice infected with HSV-1 KOS-GFP; however, viral replication in the TG of WT mice infected with HSV-1 0ΔNLS fell below the lower limit of detection afforded by PCR (Fig. 2E). Consistent with the high affinity for HSV-1 replication in the mucosal epithelium in the absence of type I IFN signaling (29), viral lytic gene expression was evident at high levels in the corneas of CD118$^{-/-}$ mice infected with either HSV-1 KOS-GFP or 0ΔNLS (Fig. 2D). However, viral gene expression in the TG of CD118$^{-/-}$ mice infected with HSV-1 0ΔNLS was equivalent to the moderate

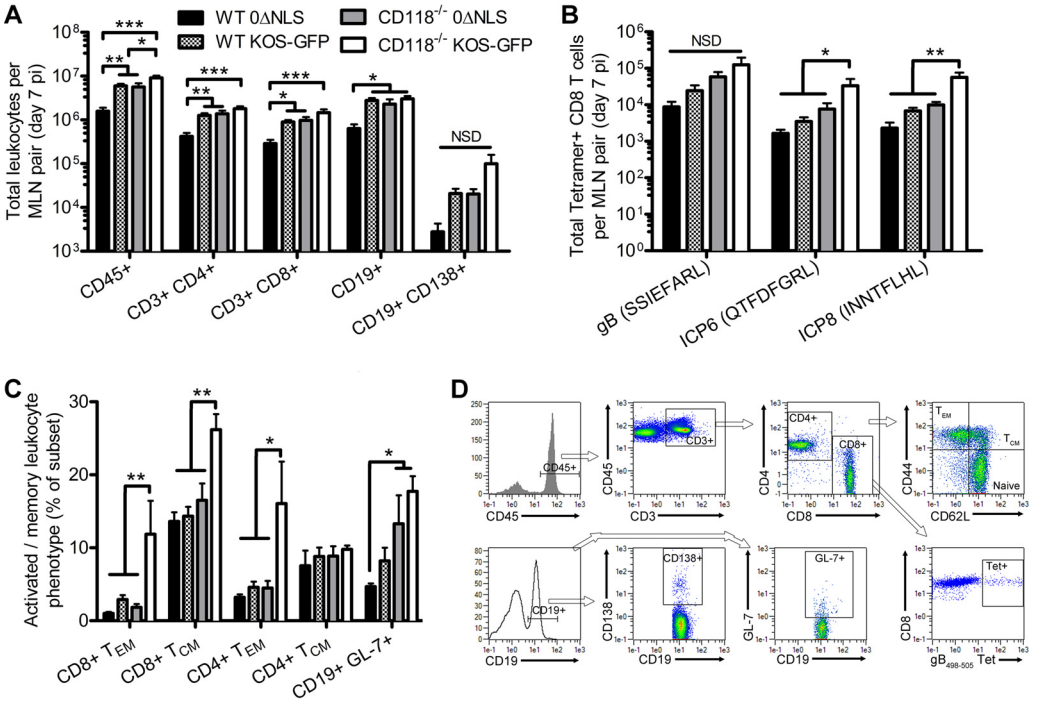

FIG 3 Impact of the ICP0 phenotype and IFN-α/β signaling on immunogenicity. Flow cytometric analysis of leukocyte populations at day 7 p.i. in the mandibular lymph nodes (MLN) of WT and CD118$^{-/-}$ mice ocularly infected with 1×10^4 PFU of HSV-1 0ΔNLS or KOS-GFP. (A) Total CD45$^+$ leukocytes, CD3$^+$ CD4$^+$/CD8$^+$ T lymphocytes, CD19$^+$ B lymphocytes, and CD19$^+$ CD138$^+$ plasmablasts. (B) Enumeration of HSV-1-specific CD8$^+$ T lymphocytes based on tetramer labeling for the top three immunodominant HSV-1 epitopes in C57BL/6 mice, including glycoprotein B (gB) and infected cell proteins 6/8 (ICP6/8). Antigen peptide sequences are listed parenthetically. (C) Evaluation of cellular activation/memory within the indicated lymphocyte subsets based on the following surface antigen expression phenotypes: CD44$^+$ CD62L$^-$ effector memory T cells (T_{EM}), CD44$^+$ CD62L$^+$ central memory T cells (T_{CM}), and GL-7$^+$ activated B cells. Data in panels A to C represent 5 to 6 mice per group (2 independent experiments); results were compared using one-way analysis of variance with Newman-Keuls multiple comparison tests. *, $P < 0.05$; **, $P < 0.01$, ***, $P < 0.001$; NSD, not statistically different. (D) Representative gating strategy for flow cytometry data. Gates were based on isotypic and/or fluorescence-minus-one controls (data not shown). Single cells with forward and side scatter properties consistent with lymphocytes (data not shown) were analyzed for surface antigen expression. The CD45$^+$ leukocyte population was selected, subgated into CD3$^+$ T cells, and subsequently subgated into CD4 and CD8 subsets (top row, first three panels). Each T cell subset was then profiled phenotypically by CD44 and CD62L expression patterns (top rightmost panel), and CD8 T cells were evaluated for reactivity with tetramers to assess HSV specificity (bottom rightmost panel). CD19$^+$ cells were selected and divided into CD138$^+$ plasmablasts and CD138$^-$ B cells (bottom row, first two panels). Activated CD19$^+$ B cells were identified by upregulation of GL-7 antigen (bottom row, third panel).

levels observed in WT mice infected with HSV-1 KOS-GFP (Fig. 2E). In contrast, CD118$^{-/-}$ mice infected with HSV-1 KOS-GFP exhibited very high levels of lytic gene expression in the TG (Fig. 2E). Consistent with the PCR data, high HSV-1 titers were observed in the corneas of CD118$^{-/-}$ mice infected with either HSV-1 0ΔNLS or KOS-GFP. Titers were also high in the TG and brainstem of CD118$^{-/-}$ mice infected with HSV-1 KOS-GFP but fell below the limit of detection in CD118$^{-/-}$ mice infected with HSV-1 0ΔNLS (Fig. 2F). Collectively, these data demonstrate that the HSV-1 0ΔNLS vaccine strain is highly attenuated with respect to its capacity to sustain productive replication *in vivo*, and thus it exhibits little to no propensity for neurovirulence in either WT or immunocompromised CD118$^{-/-}$ mice.

Though attenuated, the HSV-1 0ΔNLS vaccine strain remains highly immunogenic. Adaptive immune responses were profiled by flow cytometry in the mandibular lymph nodes (MLN) of WT and CD118$^{-/-}$ mice ocularly infected with either 0ΔNLS or KOS-GFP at day 7 p.i. This approach enabled the phenotypic resolution of total CD45$^+$ leukocytes, CD4$^+$ and CD8$^+$ T cells (CD3$^+$), CD19$^+$ B cells, and CD19$^+$ CD138$^+$ plasmablasts (Fig. 3A). The total cellularity and size of various lymphocyte subpopulations observed in the MLN of WT and CD118$^{-/-}$ mice (Fig. 3A) loosely correlated with the total viral burden at this time point (Fig. 2D and E). Generation of the virus-specific

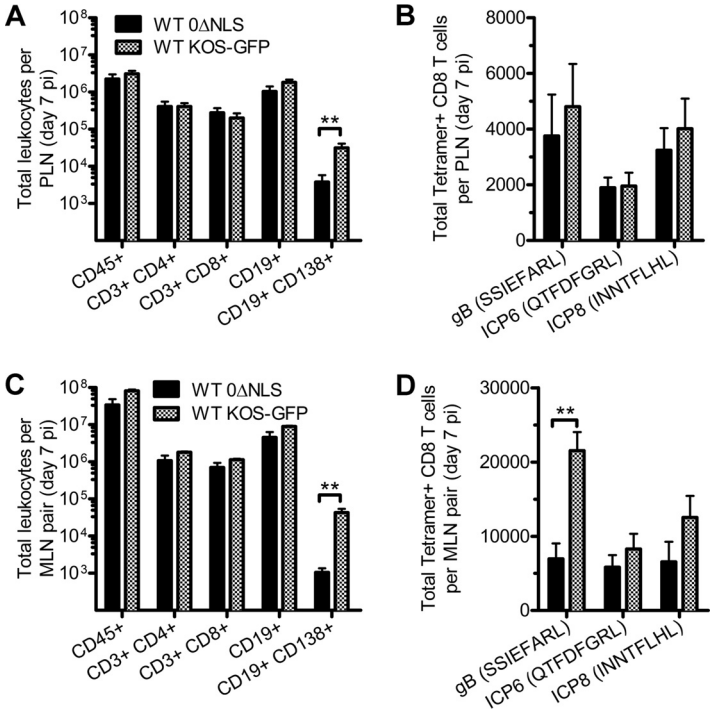

FIG 4 Subcutaneous and mucosal routes of HSV-1 0ΔNLS inoculation drive similar adaptive immune responses. WT mice were infected in the corneas or footpads with 1×10^5 PFU of HSV-1 0ΔNLS or KOS-GFP, and the respective mandibular (MLN) or popliteal (PLN) draining lymph nodes were harvested at day 7 p.i. to assess generation of adaptive cellular immunity for each inoculation route. The figure was prepared using Servier Medical Art, which is freely accessible in the public domain (http://www.servier.com) under a Creative Commons Attribution 3.0 Unported License. (A and B) Comparison of general leukocyte subsets and HSV-1-specific $CD8^+$ T cells in the PLN following footpad infection. (C and D) Comparison of general leukocyte subsets and HSV-1-specific $CD8^+$ T cells in the MLN following ocular infection. Flow cytometry gating strategies are shown in Fig. 3D. Antigen peptide sequences are listed parenthetically. Data represent 5 to 6 mice per group (2 independent experiments), and results were compared using one-way analysis of variance with Newman-Keuls multiple comparison tests (**, $P < 0.01$).

$CD8^+$ T cell response was further characterized using viral peptide-loaded major histocompatibility complex (MHC) class I tetramers for the top three immunodominant HSV-1 epitopes in C57BL/6 mice, including glycoprotein B (gB), ICP6, and ICP8 (43). Expansion of each clonal HSV-specific $CD8^+$ T cell population also correlated with total viral burden (Fig. 3B). Expression patterns of memory or activation markers were analyzed on lymphocyte subpopulations, but no intrinsic differences in the cellular adaptive immune responses were identified between WT mice infected with HSV-1 0ΔNLS and those infected with KOS-GFP. Percentages of the $CD4^+$ or $CD8^+$ T cell populations expressing effector ($CD44^+$ $CD62L^-$) or central memory ($CD44^+$ $CD62L^+$) phenotypes were equivalent among WT mice infected with HSV-1 0ΔNLS and those infected with KOS-GFP (Fig. 3C). Likewise, the percentages of B cells expressing the activation marker GL-7 were equivalent between mice infected with HSV-1 0ΔNLS and those infected with KOS-GFP (Fig. 3C). Representative dot plots for all flow cytometry data are shown in Fig. 3D. Collectively, these data indicate that the attenuated HSV-1 0ΔNLS vaccine strain drives innate and adaptive immune responses similar to those of the pseudo-wild-type HSV-1 KOS-GFP strain.

In order to assess potential tissue-specific differences in the adaptive immune responses to HSV-1 0ΔNLS and KOS-GFP, we infected WT mice in the cornea or footpad to simulate a mucosal or subcutaneous infection, respectively, and the regional draining lymph nodes were harvested at day 7 p.i. (Fig. 4A to D). Footpad and ocular infections with HSV-1 0ΔNLS and KOS-GFP yielded highly similar cellular immune responses in the regional draining lymph nodes (Fig. 4). However, the numbers of

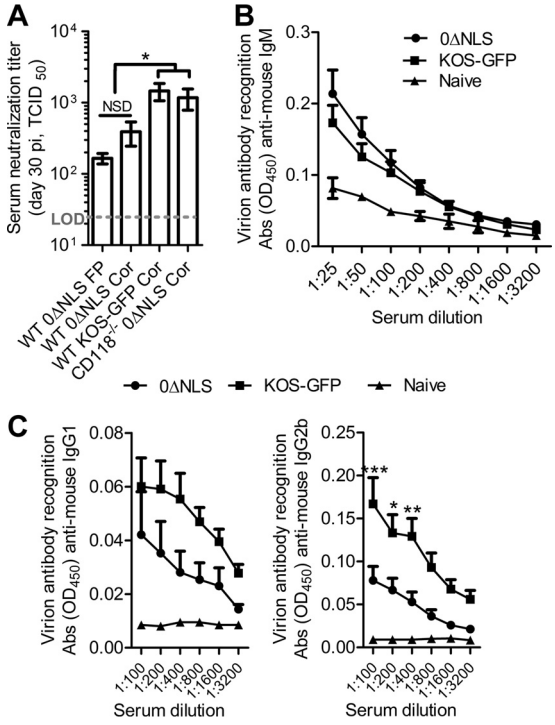

FIG 5 Humoral immune responses elicited by HSV-1 0ΔNLS and KOS-GFP infection. Mice were infected with a total of 1×10^5 PFU of HSV-1 0ΔNLS or KOS-GFP, and serum was collected at day 30 p.i. to assess humoral immunity directed against HSV-1. (A) Serum neutralization titers in WT and CD118$^{-/-}$ mice infected via the corneal (Cor) or footpad (FP) route. Virus neutralization titers were recorded for the serum dilution at which a 50% reduction of cytopathic effect was observed using the tissue culture median infective dose of 10,000 PFU of HSV-1 McKrae ($n = 11$ to 13 per group, 4 independent experiments). Bars reflect means ± SEM of results compared using one-way analysis of variance with Newman-Keuls multiple comparison tests (*, $P < 0.05$). The dashed line indicates the limit of detection (LOD). (B and C) Relative antibody recognition of plate-bound whole virions with limiting dilution analysis of IgM and IgG subtypes ($n = 8$ infected serum samples per group; 2 uninfected controls were used to establish baseline absorbance for naive serum). No HSV-specific serum IgA was detected. Data points reflect means ± SEM. Statistical differences between results with 0ΔNLS and KOS-GFP antisera were detected by two-way analysis of variance with Bonferroni posttests (*, $P < 0.05$; **, $P < 0.01$, ***, $P < 0.001$). OD_{450}, optical density at 450 nm.

CD19$^+$ CD138$^+$ plasmablasts were elevated in animals infected with HSV-1 KOS-GFP in comparison to levels in HSV-1 0ΔNLS-infected mice for both sites of inoculation (Fig. 4A and C). Additionally, the number of gB-specific CD8$^+$ T cells in the mandibular lymph nodes (MLN) of mice ocularly infected with HSV-1 KOS-GFP (Fig. 4D) was significantly elevated relative to that in HSV-1 0ΔNLS-infected mice.

Humoral immune responses were compared in mice infected with HSV-1 0ΔNLS and those infected with KOS-GFP by measuring serum neutralization titers and HSV-specific immunoglobulin levels at day 30 p.i. The ocular-versus-footpad route of virus inoculation had no effect on serum neutralizing antibody responses (Fig. 5A). In contrast, mice infected with HSV-1 KOS-GFP produced twice as much virus-neutralizing antibody as mice infected with HSV-1 0ΔNLS (Fig. 5A). Furthermore, serum neutralizing antibody titers produced in response to the HSV-1 0ΔNLS vaccine strain were equally high in CD118$^{-/-}$ mice (Fig. 5A); this finding correlates with the increased capacity of HSV-1 0ΔNLS to sustain productive viral replication in CD118$^{-/-}$ mice relative to that in WT mice (Fig. 2). No differences were observed in serum concentrations of virus-specific IgM or IgG1 in WT mice ocularly infected with HSV-1 0ΔNLS and those infected with KOS-GFP, but a slight elevation in HSV-specific IgG2b concentration was noted in mice infected with HSV-1 KOS-GFP (Fig. 5B). Consistent with prior results, our data show that the HSV-1 0ΔNLS virus is avirulent, yet it maintains a high degree of both cellular and humoral immunogenicity.

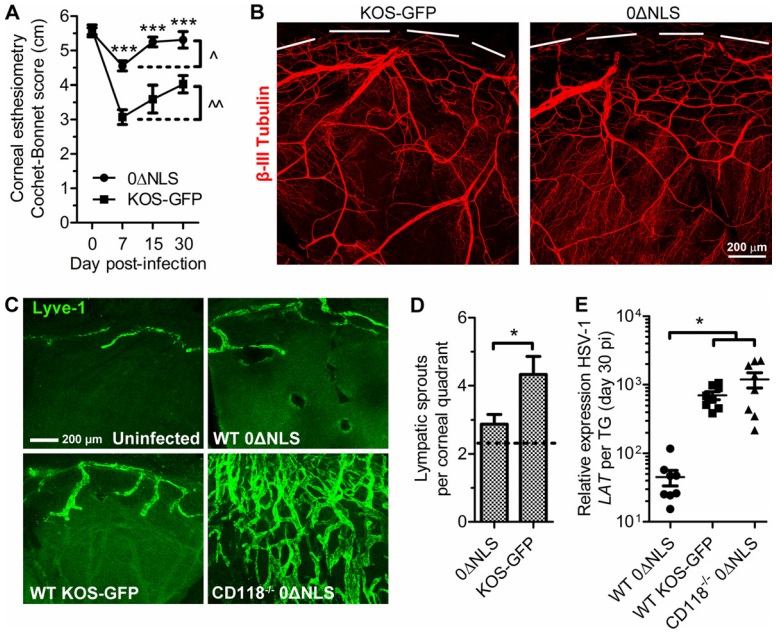

FIG 6 Longitudinal evaluation of corneal pathology and viral latency in HSV-1 0ΔNLS-infected mice. Mice were ocularly infected with 1×10^5 PFU of 0ΔNLS or KOS-GFP, and tissue was assessed for pathology or viral latency at day 30 p.i. (A) Evaluation of corneal sensation in WT mice following ocular infection (n = 12 to 28 corneas/group/time p.i.; 3 to 4 independent experiments). Asterisks indicate significant differences between results for the 0ΔNLS and KOS-GFP groups determined by two-way analysis of variance with Bonferroni posttests while carats reflect changes between days 7 and 30 p.i. within each group as determined by a Mann-Whitney U test (^, $P < 0.05$; ^^, $P < 0.01$, ***, $P < 0.001$). (B) Representative confocal images of corneal stromal nerve bundles and the fine epithelium-innervating subbasal nerve fibers labeled with βIII-tubulin antibody at day 30 p.i. (C) Representative confocal images of corneal lymphatic vessels labeled with anti-Lyve-1 antibody in healthy or infected WT and CD118$^{-/-}$ mice. (D) Quantification of the number of lymphatic vessel sprouts branching off the pericorneal limbal vasculature into the cornea proper of 0ΔNLS- and KOS-GFP-infected WT mice (n = 4 corneas/group, 2 independent experiments). *, $P < 0.05$ (Mann-Whitney U test). The dotted line reflects the number of lymphatic branches observed in healthy uninfected corneas (n = 2). (E) Quantitation of latent virus via expression of the HSV-1 latency-associated transcripts (LAT) relative to murine phosphoglycerate kinase (PGK1) expression in the TG at day 30 p.i. (n = 8 specimens per group; horizontal bars reflect means ± SEM). *, $P < 0.05$ (nonparametric Kruskal-Wallis method with Dunn's posttests).

HSV-1 0ΔNLS does not induce substantial ocular pathology but does establish a low-level latent infection. Recent evidence implicates corneal sensation loss as an important pathology associated with the host inflammatory response following ocular HSV-1 infection (44–48). Accordingly, corneal sensation was measured longitudinally following ocular infection of WT mice to determine if HSV-1 0ΔNLS elicits a pathognomonic loss of corneal sensation that is equivalent to that produced by the pseudo-wild-type HSV-1 KOS-GFP strain. Both strains induced a transient acute loss of sensation by day 7 p.i. (Fig. 6A). The sensation loss observed at day 7 p.i. in HSV-1 0ΔNLS-infected mice was mild and returned to nearly baseline levels by day 15 p.i. (Fig. 6A). However, corneal sensation loss was more severe in mice infected with HSV-1 KOS-GFP by day 7 p.i.; moreover, a partial yet incomplete recovery of corneal sensation was observed in these animals by day 30 p.i. (Fig. 6A). The functional loss of corneal sensitivity was corroborated by confocal imaging of corneal buttons in which the density of fine subbasal sensory nerve termini was noticeably reduced in corneas of mice infected with HSV-1 KOS-GFP but preserved in HSV-1 0ΔNLS-infected animals (Fig. 6B).

Corneal neovascularization is another hallmark of herpetic eye disease for which the host immune response is thought to play an important role (49–52). Accordingly, corneas were harvested from mice ocularly infected with HSV-1 0ΔNLS or KOS-GFP at day 30 p.i. and imaged by confocal microscopy to discern the potential impact HSV-1

0ΔNLS may have on corneal neovascularization (Fig. 6C). Specifically, the numbers of Lyve-1-positive lymphatic vessel sprouts extending into the corneas from the pericorneal vasculature were compared in WT and CD118$^{-/-}$ mice infected with HSV-1 0ΔNLS or KOS-GFP (Fig. 6D). No apparent differences in neovascularization were observed between HSV-1 0ΔNLS-infected and uninfected corneas; however, an increase in the number of sprouting lymphatic neovessels was observed in the corneas of HSV-1 KOS-GFP-infected WT mice at day 30 p.i. (Fig. 6D). Consistent with the high level of viral replication in corneas from CD118$^{-/-}$ mice infected with 0ΔNLS at day 7 p.i. (Fig. 2D), intense neovascularization was observed in corneas from these animals at day 30 p.i. (Fig. 6D). Therefore, in immunocompetent WT mice that retain the innate IFN-α/β signaling axis, the HSV-1 0ΔNLS vaccine strain is grossly attenuated in its capacity to cause ocular pathology in terms of either loss of corneal sensation or corneal neovascularization.

To further address the safety of the attenuated HSV-1 0ΔNLS vaccine strain, we investigated its capacity to establish a latent infection in the peripheral nervous system relative to that of the pseudoparental HSV-1 KOS-GFP. Previous studies have shown that ICP0-null strains of HSV-1 are capable of establishing latent infection but fail to reactivate efficiently (53, 54). Latency facilitates viral persistence for the life of the host by sequestering the viral genome in immune-privileged neurons. Latent HSV-1 infection is empirically defined by prolonged periods during which HSV antigen and infectious virus are not detectable, but chronic expression of the noncoding latency-associated transcripts (LAT) is observed in ganglionic neurons (55). In order to assess the extent of viral latency, trigeminal ganglia were harvested from WT and CD118$^{-/-}$ mice ocularly infected with either HSV-1 0ΔNLS or KOS-GFP at day 30 p.i., and LAT expression was evaluated by semiquantitative real-time PCR as an indirect correlate of the total burden of latent virus relative to that in uninfected ganglia. Relative LAT expression data indicate that the HSV-1 0ΔNLS virus does in fact establish a latent infection (Fig. 6E). However, our data indicate that the latent reservoir of virus is significantly diminished in WT mice infected with the HSV-1 0ΔNLS strain in comparison to the level in mice infected with HSV-1 KOS-GFP. Again, this finding is consistent with the weakened neuroinvasiveness of HSV-1 0ΔNLS (Fig. 2A) and its dearth of lytic gene expression in the TG (Fig. 2E) of immunocompetent animals during acute infection. Notably, consistent with viral replication during acute infection (Fig. 2E), the relative LAT expression exhibited by the HSV-1 0ΔNLS strain in CD118$^{-/-}$ mice mirrors that of the HSV-1 KOS-GFP strain in WT mice (Fig. 6E) at day 30 p.i. We interpret this final evidence to indicate that the homologous recombination utilized to modify the ICP0 coding sequence in the HSV-1 0ΔNLS strain did not affect the ability of the strain to express LAT or the fidelity of detection by PCR, despite the partially overlapping coding sequences of the LAT and ICP0 genes on cDNA strands of the HSV-1 genome (51, 53, 54).

DISCUSSION

Our studies conclusively demonstrate that while the HSV-1 0ΔNLS vaccine does establish a latent infection, it exhibits no propensity for neurovirulence even in mice lacking the IFN-α/β receptor. Establishment of latency by the HSV-1 0ΔNLS vaccine strain may not condemn future prospects for a 0ΔNLS vaccine trial as clinical evidence shows that the highly efficacious live-attenuated VZV vaccine also goes latent in vaccinated subjects (56). Lower viral loads induced by vaccination, as opposed to natural infection with a fully virulent strain, may account for the significantly lower occurrence of vaccine-associated VZV disease (4). Moreover, animal studies using replication-defective HSV-1 mutants demonstrate that lytic replication is not a prerequisite for the establishment of neuronal latency (57). Recent evidence suggests that HSV-1 latency may represent less of an autocratic state of quiescence than once assumed (58). Rather, HSV-1 latency is maintained on a single-cell basis by an active host immune response to successive bursts of lytic gene activity in the majority of infected neurons (59). Hence, HSV-1 latency may better reflect sustained abortive

reactivation that is regulated by the dynamics of viral genetics, total viral burden, and host immune pressure. This basal level of immune activation may contribute to the heterologous protection associated with other latent herpesvirus infections (14).

Survival of the highly immunocompromised CD118$^{-/-}$ mice following infection with HSV-1 0ΔNLS was an unexpected observation stemming from this investigation. It is well established that IFN-α/β signaling plays a critical role in inducing antiviral genes to suppress viral replication and spread in the corneal epithelium (29); however, nonmitotic sensory nerves in the ganglia are less responsive to the downstream proapoptotic effects of IFN-α/β signaling (60–62). Moreover, survival of HSV-1-infected mice lacking IFN-α/β signaling underscores the importance of two other recent mechanisms associated with host control of HSV-1, including autophagy and humoral immunity. Autophagy plays an important protective role in HSV-infected neurons as a cell-intrinsic mechanism capable of degrading viral components (63, 64). More recently, it was demonstrated that the protective effects of humoral immunity against HSV requires active participation by CD4 T cells to enable circulating antibodies to bypass the blood-nerve barrier in sensory ganglia (65). Furthermore, our data show that the HSV-1 0ΔNLS vaccine strain drives robust T and B cell responses in WT and CD118$^{-/-}$ mice (Fig. 4), leading to high antibody neutralization titers in the serum (Fig. 5A). We have previously shown that HSV-1 McKrae gains access to the draining lymph nodes and disrupts adaptive immune responses in CD118$^{-/-}$ mice (62, 66, 67); however, this is not observed with HSV-1 0ΔNLS or KOS-GFP (Fig. 4). The recent study by Iijima and Iwasaki alone has great implications for HSV-1 vaccine development (65) as the minimal-antigen immunization approaches involved in subunit vaccines may not contain the antigenic breadth required to generate protective, robust, and coordinated cellular and humoral responses essential for protection (68).

The ocular route of infection was predominately used in the present investigation to assess the safety of the HSV-1 0ΔNLS vaccine from the perspective of viral pathogenesis and tissue immunopathology although this approach would not be considered either a viable or appropriate option for vaccination in the clinic. Ocular infection is ideal for investigating HSV-1 neuropathogenesis in animal models as the corneal epithelium exhibits a much higher density of sensory nerve fibers than any other anatomic site (69). Given the proximity of sensory nerve fibers to highly susceptible epithelial cells in the cornea, HSV-1 is able to efficiently undergo neuroinvasion following ocular infection. Furthermore, the trigeminal ganglia housing the nuclei of cornea-innervating sensory nerve fibers are much larger and more easily recovered for sampling of viral content than dorsal root ganglia along the spinal cord, which are often utilized for mouse models of skin or vaginal infection. We found it of interest that expression of the lytic viral TK gene in corneas of WT animals ocularly infected with HSV-1 0ΔNLS lags behind that in mice infected with HSV-1 KOS-GFP at early time points (Fig. 1F) but is similar between the two groups by day 7 p.i. (Fig. 2D). This observation is consistent with the increased sensitivity of ICP0 mutant viruses to IFN-α/β and is corroborated by the efficient corneal replication (Fig. 2D) and neuroinvasion (Fig. 2A) of HSV-1 0ΔNLS in CD118$^{-/-}$ mice. Contrary to expectations, viral gene expression levels were comparable between HSV-1 0ΔNLS and KOS-GFP in the corneas of WT mice by day 7 postinfection (Fig. 2D). We speculate that this phenomenon is a bottleneck effect resulting from the reduced neuroinvasive efficiency of the 0ΔNLS strain as the majority of viral progeny spread to other cells in the cornea. In contrast, KOS-GFP-derived viral progeny efficiently undergo neuroinvasion to replicate in the TG (Fig. 2A and E). The sustained low-level replication of HSV-1 0ΔNLS exclusively outside the nervous system is likely a major contributing factor to its immunogenicity and lack of virulence.

Many prominent sequelae associated with ocular HSV-1 infection are attributed to an unbridled immune response. These include corneal scarring, neovascularization, and sensation loss, all of which are recapitulated in the animal model of ocular infection (11, 45, 46, 51, 70). Phylogenetic differences among virulence determinants in different HSV-1 strains are associated with various degrees of corneal neovascularization (71). In particular, the HSV-1 ICP4 protein is a major factor responsible for inducing corneal

lymphangiogenesis by driving vascular endothelial growth factor (VEGF) expression in infected corneal epithelial cells (72). As discussed previously, the HSV-1 KOS strain does not induce the same extent of corneal pathology as other strains often used for laboratory research (38–40). This was underscored by the small degree of corneal neovascularization observed in WT mice infected with HSV-1 KOS-GFP (Fig. 6C). Virulent HSV-1 strains such as McKrae have been shown to infect every layer of the cornea in CD118$^{-/-}$ mice and destroy lymphatic vessels during acute infection (29, 67). The acute death of these animals pursuant to HSV-1 infection has rendered investigating late pathology in the eye impossible until now. While the HSV-1 0ΔNLS strain replicates at high levels in the corneas of CD118$^{-/-}$ mice during acute infection (Fig. 2D and F), its lack of neurovirulence facilitates the survival of these otherwise highly susceptible mice. Whether HSV-1 0ΔNLS leads to induction or loss of corneal lymphatic vessels was not investigated in CD118$^{-/-}$ mice during acute infection; however, the robust lymphangiogenesis observed in the corneas of these mice at day 30 p.i. is consistent with a high level of VEGF-induced neovascularization. Notably, VEGF signaling has been shown to inhibit IFN-α/β signaling through ubiquitin-mediated receptor degradation, and, conversely, IFN-α/β signaling impedes angiogenesis (73). The effects of HSV-1-associated VEGF production are clear with respect to corneal neovascularization (72); however, whether HSV-1 has evolved its capacity to induce VEGF as a supplemental means of inhibiting IFN-α/β signaling remains to be explored.

Considering that the eye is classically considered an immune-privileged site, regionally localized infections may contribute to divergent adaptive immune responses. This potential was explored by comparing the cellular immune responses in the draining lymph nodes in ocular and footpad infections (Fig. 4). However, very similar cellular responses were observed between the two sites, indicating that HSV-1 infection drives immune responses that overcome ocular immune privilege. Furthermore, humoral responses were also remarkably similar for WT mice at day 30 p.i. in terms of serum neutralization titers elicited by corneal and footpad infection with HSV-1 0ΔNLS. Concerns that amplifying the host immune response to a common ocular pathogen could have a negative impact on vision abound; however, our studies indicate that prophylactic vaccination with HSV-1 0ΔNLS completely prevents HSV-associated ocular pathology (25).

The ability of prophylactic live-attenuated HSV vaccines to be avirulent yet drive a protective humoral immune response has been highlighted recently by several groups (25, 65, 74–76). Consistent with these reports, the concept that a live-attenuated HSV vaccine is a tenable option for prophylactic protection is evident. The future directions of HSV vaccine research will involve a cost-benefit analysis of live-attenuated versus subunit cocktail vaccines. Advantages of live-attenuated vaccines as demonstrated here include the activation of all phases of the immune system to generate robust humoral and cellular immune responses with antigenic breadth similar to that induced by natural infection and likely the enhanced longevity of protection in children and adolescents with no previous exposure to HSV. Moreover, live-attenuated influenza vaccines have emerged as the preferred vaccines in this age group in comparison to the trivalent inactivated vaccine, and this preference is attributed to the inferior performance of inactivated vaccines in children not previously infected with the influenza virus (77). On the other hand, concerns of genetic reversion of attenuated pathogens and their enhanced virulence in immunocompromised patients are evident. Finally, our findings collectively support the lack of virulence and safety of the HSV-1 0ΔNLS vaccine strain to evoke broad humoral and cellular responses to prevent HSV-1 associated disease, even in highly immunocompromised CD118$^{-/-}$ mice.

MATERIALS AND METHODS

Mice and viral infection. Inbred C57BL/6 wild-type (WT) mice were obtained from the Jackson Laboratory and housed in a specific-pathogen-free vivarium at the Dean McGee Eye Institute. IFN-α/β receptor-deficient (CD118$^{-/-}$) mice were bred in-house. This study was conducted according to protocols approved by the University of Oklahoma Health Sciences Center animal care and use committee. Except during measuring of corneal mechanosensory blink reflexes, animals were anesthetized by

TABLE 1 Primer sequences

Primer[a]	Sequence
HSV-1 ICP27 FWD	5′-GCATCCTTCGTGTTTGTCAT-3′
HSV-1 ICP27 REV	5′-ACCAAGGGTCGCGTAGTC-3′
HSV-1 TK FWD	5′-ATACCGACGATCTGCGACCT-3′
HSV-1 TK REV	5′-TTATTGCCGTCATAGCGCGG-3′
HSV-1 gB FWD	5′-TCTGCACCATGACCAAGTG-3′
HSV-1 gB REV	5′-TGGTGAAGGTGGTGGATATG-3′
Mu PGK1 FWD	5′-CTGACTTTGGACAAGCTGGACG-3′
Mu PGK1 REV	5′-GCAGCCTTGATCCTTTGGTTG-3′

[a]FWD, forward; gB, glycoprotein B; HSV-1, herpes simplex virus 1; ICP27, infected cell protein 27; Mu, murine; PGK1, phosphoglycerate kinase 1; REV, reverse; TK, thymidine kinase.

intraperitoneal injection with a solution of ketamine (100 mg/kg) and xylazine (6.6 mg/kg) for all procedures. For ocular infection, corneas were subjected to partial epithelial debridement using a 25-gauge needle, blotted to remove tear film, and inoculated bilaterally with a 3.0-μl drop of virus on each cornea. For intranasal and footpad infection, a 10.0-μl inoculum was administered into the nares or injected into the footpad unilaterally. All animals were immunologically naive with respect to HSV-1 prior to infection. For experiments comparing intranasal/footpad and ocular routes of infection, the combined bilateral corneal inoculum was equivalent to the intranasal inoculum or unilateral footpad injection in quantified virus PFU of HSV-1. Animals were euthanized by cardiac perfusion with 10 ml of phosphate-buffered saline (PBS) for tissue collection or by cervical dislocation upon onset of lethal encephalitis for humane concerns.

Virus strains. Virus stocks used for these studies were derived from HSV-1 strain KOS and generated by homologous recombination as described previously. Briefly, the pseudoparental HSV-1 KOS-GFP strain contains a green fluorescent protein (GFP) gene expression cassette driven by an immediate early cytomegalovirus (CMV) promoter between the HSV-1 UL26 and UL27 genes (Fig. 1A). Previous characterization of the HSV-1 KOS-GFP virus revealed no substantial defects on its behavior *in vitro* or *in vivo* (78). The attenuated HSV-1 0ΔNLS strain contains an in-frame insertion of the GFP coding sequence on the immediate early ICP0 gene between codons 104 and 105 on exon 2 and lacks the canonical nuclear localization signal (NLS) motif, R-P-R-K-R-R, encoded by amino acids 501 to 508 on exon 3 (Fig. 1B). The HSV-1 KOS-GFP and 0ΔNLS strains were propagated on Vero (ATCC) and L7 cell lines, respectively. The L7 cell line is an ICP0-complementing Vero cell line that supports the optimal growth of the attenuated HSV-1 0ΔNLS strain (79). The pseudoparental HSV-1 KOS-GFP strain was chosen for comparison to HSV-1 0ΔNLS, which expresses a chimeric mutant ICP0-GFP protein, for live-animal imaging and as a control to assess the consequence of inserting the GFP coding sequence on HSV-1 virulence and disease pathogenesis.

Host antiviral gene array. For analysis of host and virus gene expression, tissue was harvested at the times postinfection (p.i.) indicated in the figure legends, and RNA was isolated and converted to cDNA as described previously (80). Amplification of host antiviral genes was conducted by real-time PCR using PrimePCR technology (Bio-Rad) according to the manufacturer's directions on a CFX-Connect thermocycler (Bio-Rad), with relative expression standardized to that of uninfected controls and calculated by the $2^{-\Delta\Delta CT}$ (where *CT* is threshold cycle) method, with *GAPDH* (glyceraldehyde 3-phosphate dehydrogenase) and *TBP* (TATA box-binding protein) used as reference genes. Array data were transformed into a heat map using the National Cancer Institute's CIMminer tool, which is freely accessible online (https://discover.nci.nih.gov/cimminer/), with hierarchical clustering determined using the Euclidean distance average linkage algorithm. Principal-component analysis of the multivariate array data was performed using the open access ClustVis tool (http://biit.cs.ut.ee/clustvis/) as described previously (81).

Virus quantification. Viral gene expression was assessed by semiquantitative real-time PCR, and HSV-1 titers were quantified by plaque assay. Viral gene expression in excised corneas and trigeminal ganglia was evaluated as described previously (25). Briefly, HSV-1 gene expression was calculated using the $2^{-\Delta\Delta CT}$ method relative to murine levels of *PGK1* (phosphoglycerate kinase 1) expression and standardized to levels in uninfected controls for both lytic and latent viral genes. Primers for HSV-1 and host genes are listed in Table 1. Titers of infectious virus were determined by plaque assay on U2OS osteosarcoma cells (American Type Culture Collection), which discernibly complement replication of HSV-1 ICP0-null mutant strains (82–85). The U2OS cell line was subcultured with Dulbecco's modified Eagle medium (DMEM) supplemented with 10% heat-inactivated fetal bovine serum, 1× antibiotic/antimycotic, and 10 μg/ml gentamicin (Life Technologies), which is here designated complete medium. Briefly, clarified homogenates from infected tissues were incubated on confluent U2OS cell monolayers in 96-well microtiter plates for 1 h, decanted, and replaced with complete medium containing 0.5% methylcellulose. Viral plaques were counted 44 to 48 h later.

Serum immunoassays. Humoral responses to HSV-1 were evaluated by serum neutralization assay and further profiled by enzyme-linked immunosorbent assay (ELISA) to assess the antibody isotypes associated with virion binding. Whole blood was obtained from the facial vein of mice at day 30 p.i., and serum was fractionated using Microtainer serum separator tubes (Becton Dickinson) as previously described (25). Neutralization assays were performed by incubating serial dilutions of serum with 10,000 PFU of HSV-1 (strain McKrae) in the presence of guinea pig complement for 1 h, exposing the mixture

to confluent monolayers of Vero cells (American Type Culture Collection) in 96-well microtiter plates for 1 h, and replacing the medium with RPMI 1640 medium supplemented with 10% heat-inactivated fetal bovine serum, 1× antibiotic/antimycotic, and 10 μg/ml gentamicin (Life Technologies), i.e., complete RPMI medium, as previously described (25). Neutralizing serum titers were determined 24 h after exposure and are reported as the reciprocal dilution upon 50% reduction of cytopathic effect using the empirically determined median tissue culture infectious dose ($TCID_{50}$) of HSV-1 strain McKrae.

Isotype-specific HSV-1 antibody titers were measured using HSV-1 virions as described previously (86). Briefly, purified virions were adsorbed onto 96-well microtiter plates in carbonate buffer (pH 9.6) and incubated overnight at room temperature. Excess antigen was removed by washing wells three times with PBS-Tween, serial dilutions of mouse serum (naive and infected) were added to the wells, and the plates were incubated at room temperature for 2 h. Wells were washed three times with PBS-Tween and then incubated with alkaline phosphatase-conjugated anti-mouse IgA, IgM, IgG1, or IgG2b detection antibodies (1:2,000 dilution; Southern Biotechnology, Birmingham, AL) for 2 h at room temperature. Wells were then washed three times with PBS-Tween and incubated with para-nitrophenyl phosphate substrate for 60 to 120 min at room temperature. The optical density at 450 nm was measured using a Clariostar microplate reader (BMG Labtech, Ortenberg, Germany) with background correction at the 540-nm wavelength.

Corneal imaging and pathology. An Olympus MVX10 MacroZoom fluorescence microscope was used for *in vivo* imaging of GFP-expressing virus on corneal lesions of infected mice during acute infection (Fig. 1E). Corneas were prepared for histological analysis of corneal innervation and vascularity as previously described (44, 72). Immunolabeled corneal flat mounts were imaged using an Olympus FV1200 confocal microscope. Corneal mechanosensation was measured using a handheld Cochet-Bonnet esthesiometer (Luneau Technology), as previously described (44).

Flow cytometry. Adaptive immune responses were assessed by flow cytometry at day 7 p.i. using the mandibular lymph nodes (MLN) for ocular infections and the corresponding popliteal lymph node (PLN) for footpad infections. Lymph nodes were macerated into single-cell suspensions over a 40-μm-pore-size mesh in complete medium. Fluorochrome-conjugated antibodies were purchased from eBioscience and Tonbo Biosciences. Mouse MHC class I K^b tetramers were provided by the NIH Tetramer Core Facility for identification of HSV-1-specific $CD8^+$ T cells. Cells were labeled and washed in PBS containing 1% bovine serum albumin as described previously (25). Samples were analyzed on a MACSQuant-10 flow cytometer with MacsQuantify software (Miltenyi Biotec). Gating strategies shown are based on fluorescence-minus-one and isotype controls for antibody labeling and uninfected control samples for tetramer-positive $CD8^+$ T cells.

Statistical analysis. GraphPad Prism, version 5, was used for statistical analysis. Data reflect means ± standard errors of the means (SEM). Statistical tests used for analysis are described in each figure legend.

ACKNOWLEDGMENTS

We thank the Dean McGee Eye Institute vivarium staff for maintaining animal colonies and Helen Rosenberg for providing the initial breeders of our $CD118^{-/-}$ mouse colony.

The content of the manuscript is solely the responsibility of the authors and does not necessarily represent the official views of the National Institutes of health or the National Eye Institute.

D.J.R. designed and conducted experiments, analyzed all data, and prepared the manuscript; M.M.C. assisted with experiments; A.J.C.-E. performed confocal imaging of corneal nerves; W.P.H. provided the 0ΔNLS and KOS-GFP virus strains and critiqued the manuscript; and D.J.J.C. performed antibody recognition assays and supervised all work.

D.J.R., M.M.C., A.J.C.-E., and D.J.J.C have no conflicts of interest to report. W.P.H. is a coauthor on U.S. patent 8802109, which describes the use of herpes simplex virus mutant ICP0 in the design of a live-attenuated HSV-2 vaccine strain. In addition, W.P.H. is a cofounder of Rational Vaccines, Inc., which has licensed U.S. patents 77856605 and 8802109.

This work was supported by National Institutes of Health (NIH) Grants R01 EY021238, P30 EY021725, and T32 EY023202. Additional support was provided by an unrestricted grant from Research to Prevent Blindness.

We dedicate this work to our close colleague and friend, Bryan M. Gebhardt, who passed away 1 December 2016. Gebhardt was instrumental in establishing the career path of D.J.J.C. and W.P.H.

REFERENCES

1. Plotkin SA. 2005. Vaccines: past, present and future. Nat Med 11(4 Suppl):S5–S11.

2. Koff WC, Burton DR, Johnson PR, Walker BD, King CR, Nabel GJ, Ahmed R, Bhan MK, Plotkin SA. 2013. Accelerating next-generation vaccine

development for global disease prevention. Science 340:1232910. https://doi.org/10.1126/science.1232910.
3. Virgin HW, Wherry EJ, Ahmed R. 2009. Redefining chronic viral infection. Cell 138:30–50. https://doi.org/10.1016/j.cell.2009.06.036.
4. Schmid DS, Jumaan AO. 2010. Impact of varicella vaccine on varicella-zoster virus dynamics. Clin Microbiol Rev 23:202–217. https://doi.org/10.1128/CMR.00031-09.
5. Shapiro ED, Vazquez M, Esposito D, Holabird N, Steinberg SP, Dziura J, LaRussa PS, Gershon AA. 2011. Effectiveness of 2 doses of varicella vaccine in children. J Infect Dis 203:312–315. https://doi.org/10.1093/infdis/jiq052.
6. Leung J, Harpaz R. 2016. Impact of the maturing varicella vaccination program on varicella and related outcomes in the United States: 1994–2012. J Pediatr Infect Dis Soc 5:395–402. https://doi.org/10.1093/jpids/piv044.
7. Royer DJ, Cohen AW, Carr DJ. 2015. The current state of vaccine development for ocular HSV-1 infection. Expert Rev Ophthalmol 10:113–126. https://doi.org/10.1586/17469899.2015.1004315.
8. Nguyen LH, Knipe DM, Finberg RW. 1992. Replication-defective mutants of herpes simplex virus (HSV) induce cellular immunity and protect against lethal HSV infection. J Virol 66:7067–7072.
9. Hoshino Y, Dalai SK, Wang K, Pesnicak L, Lau TY, Knipe DM, Cohen JI, Straus SE. 2005. Comparative efficacy and immunogenicity of replication-defective, recombinant glycoprotein, and DNA vaccines for herpes simplex virus 2 infections in mice and guinea pigs. J Virol 79:410–418. https://doi.org/10.1128/JVI.79.1.410-418.2005.
10. Morello CS, Kraynyak KA, Levinson MS, Chen Z, Lee K-F, Spector DH. 2012. Inactivated HSV-2 in MPL/alum adjuvant provides nearly complete protection against genital infection and shedding following long term challenge and rechallenge. Vaccine 30:6541–6550. https://doi.org/10.1016/j.vaccine.2012.08.049.
11. Farooq AV, Shukla D. 2012. Herpes simplex epithelial and stromal keratitis: an epidemiologic update. Surv Ophthalmol 57:448–462. https://doi.org/10.1016/j.survophthal.2012.01.005.
12. Belshe RB, Leone PA, Bernstein DI, Wald A, Levin MJ, Stapleton JT, Gorfinkel I, Morrow RLA, Ewell MG, Stokes-Riner A, Dubin G, Heineman TC, Schulte JM, Deal CD. 2012. Efficacy results of a trial of a herpes simplex vaccine. N Engl J Med 366:34–43. https://doi.org/10.1056/NEJMoa1103151.
13. Steiner I. 2011. Herpes simplex virus encephalitis: new infection or reactivation? Curr Opin Neurol 24:268–274. https://doi.org/10.1097/WCO.0b013e328346be6f.
14. Barton ES, White DW, Cathelyn JS, Brett-McClellan KA, Engle M, Diamond MS, Miller VL, Virgin HW. 2007. Herpesvirus latency confers symbiotic protection from bacterial infection. Nature 447:326–329. https://doi.org/10.1038/nature05762.
15. Duerkop BA, Hooper LV. 2013. Resident viruses and their interactions with the immune system. Nat Immunol 14:654–659. https://doi.org/10.1038/ni.2614.
16. Virgin HW. 2014. The virome in mammalian physiology and disease. Cell 157:142–150. https://doi.org/10.1016/j.cell.2014.02.032.
17. Kernbauer E, Ding Y, Cadwell K. 2014. An enteric virus can replace the beneficial function of commensal bacteria. Nature 516:94–98. https://doi.org/10.1038/nature13960.
18. Goodridge HS, Ahmed SS, Curtis N, Kollmann TR, Levy O, Netea MG, Pollard AJ, van Crevel R, Wilson CB. 2016. Harnessing the beneficial heterologous effects of vaccination. Nat Rev Immunol 16:392–400. https://doi.org/10.1038/nri.2016.43.
19. Benn CS, Fisker AB, Whittle HC, Aaby P. 2016. Revaccination with live attenuated vaccines confer additional beneficial nonspecific effects on overall survival: a review. EBioMedicine 10:312–317. https://doi.org/10.1016/j.ebiom.2016.07.016.
20. Pulendran B, Ahmed R. 2011. Immunological mechanisms of vaccination. Nat Immunol 12:509–517.
21. McNab F, Mayer-Barber K, Sher A, Wack A, O'Garra A. 2015. Type I interferons in infectious disease. Nat Rev Immunol 15:87–103. https://doi.org/10.1038/nri3787.
22. Crouse J, Kalinke U, Oxenius A. 2015. Regulation of antiviral T cell responses by type I interferons. Nat Rev Immunol 15:231–242. https://doi.org/10.1038/nri3806.
23. Carroll EC, Jin L, Mori A, Muñoz-Wolf N, Oleszycka E, Moran HBT, Mansouri S, McEntee CP, Lambe E, Agger EM, Andersen P, Cunningham C, Hertzog P, Fitzgerald KA, Bowie AG, Lavelle EC. 2016. The vaccine adjuvant chitosan promotes cellular immunity via DNA sensor cGAS-STING-dependent induction of type I interferons. Immunity 44:597–608. https://doi.org/10.1016/j.immuni.2016.02.004.
24. Antoine TE, Hadigal SR, Yakoub AM, Mishra YK, Bhattacharya P, Haddad C, Valyi-Nagy T, Adelung R, Prabhakar BS, Shukla D. 2016. Intravaginal zinc oxide tetrapod nanoparticles as novel immunoprotective agents against genital herpes. J Immunol 196:4566–4575. https://doi.org/10.4049/jimmunol.1502373.
25. Royer DJ, Gurung HR, Jinkins JK, Geltz JJ, Wu JL, Halford WP, Carr DJJ. 2016. A highly efficacious herpes simplex virus 1 vaccine blocks viral pathogenesis and prevents corneal immunopathology via humoral immunity. J Virol 90:5514–5529. https://doi.org/10.1128/JVI.00517-16.
26. Smith MC, Boutell C, Davido DJ. 2011. HSV-1 ICP0: paving the way for viral replication. Future Virol 6:421–429. https://doi.org/10.2217/fvl.11.24.
27. Austin BA, James C, Silverman RH, Carr DJJ. 2005. Critical role for the oligoadenylate synthetase/RNase L pathway in response to IFN-beta during acute ocular herpes simplex virus type 1 infection. J Immunol 175:1100–1106. https://doi.org/10.4049/jimmunol.175.2.1100.
28. Yordy B, Iijima N, Huttner A, Leib D, Iwasaki A. 2012. A neuron-specific role for autophagy in antiviral defense against herpes simplex virus. Cell Host Microbe 12:334–345. https://doi.org/10.1016/j.chom.2012.07.013.
29. Royer DJ, Carr DJJ. 2016. A STING-dependent innate-sensing pathway mediates resistance to corneal HSV-1 infection via upregulation of the antiviral effector tetherin. Mucosal Immunol 9:1065–1075. https://doi.org/10.1038/mi.2015.124.
30. Leib DA, Machalek MA, Williams BR, Silverman RH, Virgin HW. 2000. Specific phenotypic restoration of an attenuated virus by knockout of a host resistance gene. Proc Natl Acad Sci U S A 97:6097–6101. https://doi.org/10.1073/pnas.100415697.
31. Zheng X, Silverman RH, Zhou A, Goto T, Kwon BS, Kaufman HE, Hill JM. 2001. Increased severity of HSV-1 keratitis and mortality in mice lacking the 2-5A-dependent RNase L gene. Invest Ophthalmol Vis Sci 42:120–126.
32. Sobol PT, Mossman KL. 2006. ICP0 prevents RNase L-independent rRNA cleavage in herpes simplex virus type 1-infected cells. J Virol 80:218–225. https://doi.org/10.1128/JVI.80.1.218-225.2006.
33. Han X, Lundberg P, Tanamachi B, Openshaw H, Longmate J, Cantin E. 2001. Gender influences herpes simplex virus type 1 infection in normal and gamma interferon-mutant mice. J Virol 75:3048–3052. https://doi.org/10.1128/JVI.75.6.3048-3052.2001.
34. Lundberg P, Welander P, Openshaw H, Nalbandian C, Edwards C, Moldawer L, Cantin E. 2003. A locus on mouse chromosome 6 that determines resistance to herpes simplex virus also influences reactivation, while an unlinked locus augments resistance of female mice. J Virol 77:11661–11673. https://doi.org/10.1128/JVI.77.21.11661-11673.2003.
35. Knoblich A, Görtz J, Härle-Grupp V, Falke D. 1983. Kinetics and genetics of herpes simplex virus-induced antibody formation in mice. Infect Immun 39:15–23.
36. Klein SL, Flanagan KL. 2016. Sex differences in immune responses. Nat Rev Immunol 16:626–638. https://doi.org/10.1038/nri.2016.90.
37. Conrady CD, Zheng M, van Rooijen N, Drevets DA, Royer D, Alleman A, Carr DJJ. 2013. Microglia and a functional type I IFN pathway are required to counter HSV-1-driven brain lateral ventricle enlargement and encephalitis. J Immunol 190:2807–2817. https://doi.org/10.4049/jimmunol.1203265.
38. Sawtell NM, Poon DK, Tansky CS, Thompson RL. 1998. The latent herpes simplex virus type 1 genome copy number in individual neurons is virus strain specific and correlates with reactivation. J Virol 72:5343–5350.
39. Wang H, Davido DJ, Morrison LA. 2013. HSV-1 strain McKrae is more neuroinvasive than HSV-1 KOS after corneal or vaginal inoculation in mice. Virus Res 173:436–440. https://doi.org/10.1016/j.virusres.2013.01.001.
40. Macdonald SJ, Mostafa HH, Morrison LA, Davido DJ. 2012. Genome sequence of herpes simplex virus 1 strain KOS. J Virol 86:6371–6372. https://doi.org/10.1128/JVI.00646-12.
41. Yao H-W, Ling P, Chen S-H, Tung Y-Y, Chen S-H. 2012. Factors affecting herpes simplex virus reactivation from the explanted mouse brain. Virology 433:116–123. https://doi.org/10.1016/j.virol.2012.07.018.
42. Kodukula P, Liu T, Rooijen NV, Jager MJ, Hendricks RL. 1999. Macrophage control of herpes simplex virus type 1 replication in the peripheral nervous system. J Immunol 162:2895–2905.
43. St Leger AJ, Peters B, Sidney J, Sette A, Hendricks RL. 2011. Defining the herpes simplex virus-specific $CD8^+$ T cell repertoire in C57BL/6 mice. J Immunol 186:3927–3933. https://doi.org/10.4049/jimmunol.1003735.
44. Chucair-Elliott AJ, Zheng M, Carr DJJ. 2015. Degeneration and regener-

ation of corneal nerves in response to HSV-1 infection. Invest Ophthalmol Vis Sci 56:1097–1107. https://doi.org/10.1167/iovs.14-15596.
45. Hamrah P, Cruzat A, Dastjerdi MH, Zheng L, Shahatit BM, Bayhan HA, Dana R, Pavan-Langston D. 2010. Corneal sensation and subbasal nerve alterations in patients with herpes simplex keratitis: an in vivo confocal microscopy study. Ophthalmology 117:1930–1936. https://doi.org/10.1016/j.ophtha.2010.07.010.
46. Yun H, Rowe AM, Lathrop KL, Harvey SAK, Hendricks RL. 2014. Reversible nerve damage and corneal pathology in murine herpes simplex stromal keratitis. J Virol 88:7870–7880. https://doi.org/10.1128/JVI.01146-14.
47. Yun H, Lathrop KL, Hendricks RL. 2016. A central role for sympathetic nerves in herpes stromal keratitis in mice. Invest Ophthalmol Vis Sci 57:1749–1756. https://doi.org/10.1167/iovs.16-19183.
48. Chucair-Elliott AJ, Jinkins J, Carr MM, Carr DJJ. 2016. IL-6 contributes to corneal nerve degeneration after herpes simplex virus type I infection. Am J Pathol 186:2665–2678. https://doi.org/10.1016/j.ajpath.2016.06.007.
49. Bryant-Hudson KM, Gurung HR, Zheng M, Carr DJJ. 2014. Tumor necrosis factor alpha and interleukin-6 facilitate corneal lymphangiogenesis in response to herpes simplex virus 1 infection. J Virol 88:14451–14457. https://doi.org/10.1128/JVI.01841-14.
50. Rogge M, Yin X-T, Godfrey L, Lakireddy P, Potter CA, Del Rosso CR, Stuart PM. 2015. Therapeutic use of soluble Fas ligand ameliorates acute and recurrent herpetic stromal keratitis in mice. Invest Ophthalmol Vis Sci 56:6377–6386. https://doi.org/10.1167/iovs.15-16588.
51. Park PJ, Chang M, Garg N, Zhu J, Chang J-H, Shukla D. 2015. Corneal lymphangiogenesis in herpetic stromal keratitis. Surv Ophthalmol 60:60–71. https://doi.org/10.1016/j.survophthal.2014.06.001.
52. Gimenez F, Mulik S, Veiga-Parga T, Bhela S, Rouse BT. 2015. Robo 4 counteracts angiogenesis in herpetic stromal keratitis. PLoS One 10:e0141925. https://doi.org/10.1371/journal.pone.0141925.
53. Halford WP, Schaffer PA. 2000. Optimized viral dose and transient immunosuppression enable herpes simplex virus ICP0-null mutants to establish wild-type levels of latency in vivo. J Virol 74:5957–5967. https://doi.org/10.1128/JVI.74.13.5957-5967.2000.
54. Halford WP, Schaffer PA. 2001. ICP0 is required for efficient reactivation of herpes simplex virus type 1 from neuronal latency. J Virol 75:3240–3249. https://doi.org/10.1128/JVI.75.7.3240-3249.2001.
55. Block TM, Hill JM. 1997. The latency associated transcripts (LAT) of herpes simplex virus: still no end in sight. J Neurovirol 3:313–321. https://doi.org/10.3109/13550289709030745.
56. Weinert LA, Depledge DP, Kundu S, Gershon AA, Nichols RA, Balloux F, Welch JJ, Breuer J. 2015. Rates of vaccine evolution show strong effects of latency: implications for varicella zoster virus epidemiology. Mol Biol Evol 32:1020–1028. https://doi.org/10.1093/molbev/msu406.
57. Katz JP, Bodin ET, Coen DM. 1990. Quantitative polymerase chain reaction analysis of herpes simplex virus DNA in ganglia of mice infected with replication-incompetent mutants. J Virol 64:4288–4295.
58. Menendez CM, Jinkins JK, Carr DJJ. 2016. Resident T cells are unable to control herpes simplex virus-1 activity in the brain ependymal region during latency. J Immunol 197:1262–1275. https://doi.org/10.4049/jimmunol.1600207.
59. Ma JZ, Russell TA, Spelman T, Carbone FR, Tscharke DC. 2014. Lytic gene expression is frequent in HSV-1 latent infection and correlates with the engagement of a cell-intrinsic transcriptional response. PLoS Pathog 10:e1004237. https://doi.org/10.1371/journal.ppat.1004237.
60. Chawla-Sarkar M, Lindner DJ, Liu Y-F, Williams BR, Sen GC, Silverman RH, Borden EC. 2003. Apoptosis and interferons: role of interferon-stimulated genes as mediators of apoptosis. Apoptosis 8:237–249. https://doi.org/10.1023/A:1023668705040.
61. Rosato PC, Leib DA. 2015. Neuronal interferon signaling is required for protection against herpes simplex virus replication and pathogenesis. PLoS Pathog 11:e1005028. https://doi.org/10.1371/journal.ppat.1005028.
62. Royer DJ, Conrady CD, Carr DJJ. 2016. Herpesvirus-associated lymphadenitis distorts fibroblastic reticular cell microarchitecture and attenuates CD8 T cell responses to neurotropic infection in mice lacking the STING-IFN-α/β defense pathways. J Immunol 197:2338–2352. https://doi.org/10.4049/jimmunol.1600574.
63. Orvedahl A, Alexander D, Tallóczy Z, Sun Q, Wei Y, Zhang W, Burns D, Leib DA, Levine B. 2007. HSV-1 ICP34.5 confers neurovirulence by targeting the Beclin 1 autophagy protein. Cell Host Microbe 1:23–35. https://doi.org/10.1016/j.chom.2006.12.001.
64. Parker ZM, Murphy AA, Leib DA. 2015. Role of the DNA Sensor STING in protection from lethal infection following corneal and intracerebral challenge with herpes simplex virus 1. J Virol 89:11080–11091. https://doi.org/10.1128/JVI.00954-15.
65. Iijima N, Iwasaki A. 2016. Access of protective antiviral antibody to neuronal tissues requires CD4 T-cell help. Nature 533:552–556. https://doi.org/10.1038/nature17979.
66. Conrady CD, Thapa M, Wuest T, Carr DJJ. 2009. Loss of mandibular lymph node integrity is associated with an increase in sensitivity to HSV-1 infection in CD118-deficient mice. J Immunol 182:3678–3687. https://doi.org/10.4049/jimmunol.0803878.
67. Bryant-Hudson KM, Chucair-Elliott AJ, Conrady CD, Cohen A, Zheng M, Carr DJJ. 2013. HSV-1 targets lymphatic vessels in the eye and draining lymph node of mice leading to edema in the absence of a functional type I interferon response. Am J Pathol 183:1233–1242. https://doi.org/10.1016/j.ajpath.2013.06.014.
68. Halford WP. 2014. Antigenic breadth: a missing ingredient in HSV-2 subunit vaccines? Expert Rev Vaccines 13:691–710. https://doi.org/10.1586/14760584.2014.910121.
69. Schwend T, Lwigale PY, Conrad GW. 2012. Nerve repulsion by the lens and cornea during cornea innervation is dependent on Robo-Slit signaling and diminishes with neuron age. Dev Biol 363:115–127. https://doi.org/10.1016/j.ydbio.2011.12.039.
70. Vega JL, Keino H, Masli S. 2009. Surgical denervation of ocular sympathetic afferents decreases local transforming growth factor-β and abolishes immune privilege. Am J Pathol 175:1218–1225. https://doi.org/10.2353/ajpath.2009.090264.
71. Lee K, Kolb AW, Larsen I, Craven M, Brandt CR. 2016. Mapping murine corneal neovascularization and weight loss virulence determinants in the herpes simplex virus 1 genome and the detection of an epistatic interaction between the UL and IRS/US regions. J Virol 90:8115–8131. https://doi.org/10.1128/JVI.00821-16.
72. Wuest TR, Carr DJJ. 2010. VEGF-A expression by HSV-1-infected cells drives corneal lymphangiogenesis. J Exp Med 207:101–115. https://doi.org/10.1084/jem.20091385.
73. Zheng H, Qian J, Carbone CJ, Leu NA, Baker DP, Fuchs SY. 2011. Vascular endothelial growth factor-induced elimination of the type 1 interferon receptor is required for efficient angiogenesis. Blood 118:4003–4006. https://doi.org/10.1182/blood-2011-06-359745.
74. Halford WP, Püschel R, Gershburg E, Wilber A, Gershburg S, Rakowski B. 2011. A live-attenuated HSV-2 ICP0 virus elicits 10 to 100 times greater protection against genital herpes than a glycoprotein D subunit vaccine. PLoS One 6:e17748. https://doi.org/10.1371/journal.pone.0017748.
75. Petro C, González PA, Cheshenko N, Jandl T, Khajoueinejad N, Bénard A, Sengupta M, Herold BC, Jacobs WR. 2015. Herpes simplex type 2 virus deleted in glycoprotein D protects against vaginal, skin and neural disease. eLife 4:e06054. https://doi.org/10.7554/eLife.06054.
76. Petro CD, Weinrick B, Khajoueinejad N, Burn C, Sellers R, Jacobs WR, Herold BC. 2016. HSV-2 ΔgD elicits FcγR-effector antibodies that protect against clinical isolates. JCI Insight 1:e88529. https://doi.org/10.1172/jci.insight.88529.
77. Mohn KG-I, Bredholt G, Brokstad KA, Pathirana RD, Aarstad HJ, Tondel C, Cox RJ. 2015. Longevity of B-cell and T-cell responses after live attenuated influenza vaccination in children. J Infect Dis 211:1541–1549. https://doi.org/10.1093/infdis/jiu654.
78. Balliet JW, Kushnir AS, Schaffer PA. 2007. Construction and characterization of a herpes simplex virus type I recombinant expressing green fluorescent protein: acute phase replication and reactivation in mice. Virology 361:372–383. https://doi.org/10.1016/j.virol.2006.11.022.
79. Samaniego LA, Wu N, DeLuca NA. 1997. The herpes simplex virus immediate-early protein ICP0 affects transcription from the viral genome and infected-cell survival in the absence of ICP4 and ICP27. J Virol 71:4614–4625.
80. Conrady CD, Zheng M, Fitzgerald KA, Liu C, Carr DJJ. 2012. Resistance to HSV-1 infection in the epithelium resides with the novel innate sensor, IFI-16. Mucosal Immunol 5:173–183. https://doi.org/10.1038/mi.2011.63.
81. Metsalu T, Vilo J. 2015. ClustVis: a web tool for visualizing clustering of multivariate data using principal component analysis and heatmap. Nucleic Acids Res 43:W566–W570. https://doi.org/10.1093/nar/gkv468.
82. Yao F, Schaffer PA. 1995. An activity specified by the osteosarcoma line U2OS can substitute functionally for ICP0, a major regulatory protein of herpes simplex virus type 1. J Virol 69:6249–6258.
83. Mossman KL, Saffran HA, Smiley JR. 2000. Herpes simplex virus ICP0

mutants are hypersensitive to interferon. J Virol 74:2052–2056. https://doi.org/10.1128/JVI.74.4.2052-2056.2000.
84. Everett RD, Boutell C, Orr A. 2004. Phenotype of a herpes simplex virus type 1 mutant that fails to express immediate-early regulatory protein ICP0. J Virol 78:1763–1774. https://doi.org/10.1128/JVI.78.4.1763-1774.2004.
85. Gu H, Roizman B. 2007. Herpes simplex virus-infected cell protein 0 blocks the silencing of viral DNA by dissociating histone deacetylases from the CoREST-REST complex. Proc Natl Acad Sci U S A 104:17134–17139. https://doi.org/10.1073/pnas.0707266104.
86. Halford WP, Veress LA, Gebhardt BM, Carr DJ. 1997. Innate and acquired immunity to herpes simplex virus type 1. Virology 236:328–337. https://doi.org/10.1006/viro.1997.8738.